

8-5-1985

## Contribution of Scanning Electron Microscopy and Associated Analytical Techniques to the Study of Atherosclerotic Disease

R. Laschi  
*University of Bologna*

Follow this and additional works at: <https://digitalcommons.usu.edu/electron>



Part of the [Biology Commons](#)

---

### Recommended Citation

Laschi, R. (1985) "Contribution of Scanning Electron Microscopy and Associated Analytical Techniques to the Study of Atherosclerotic Disease," *Scanning Electron Microscopy*. Vol. 1985 : No. 3 , Article 32.

Available at: <https://digitalcommons.usu.edu/electron/vol1985/iss3/32>

This Article is brought to you for free and open access by the Western Dairy Center at DigitalCommons@USU. It has been accepted for inclusion in Scanning Electron Microscopy by an authorized administrator of DigitalCommons@USU. For more information, please contact [digitalcommons@usu.edu](mailto:digitalcommons@usu.edu).



CONTRIBUTION OF SCANNING ELECTRON MICROSCOPY AND ASSOCIATED ANALYTICAL  
TECHNIQUES TO THE STUDY OF ATHEROSCLEROTIC DISEASE

R. Laschi

Institute of Clinical Electron Microscopy, University of Bologna,  
Italy

(Paper received February 07, 1985; manuscript received August 05, 1985)

Abstract

Human carotid atheroma has been examined by scanning electron microscopy (SEM) utilizing both secondary and backscattered electron detectors and transmission electron microscopy (TEM) both at conventional and high voltage.

Different cytochemical techniques have been used to map elastic fibers, proteoglycans, calcium, non esterified cholesterol. By immunocytochemistry the distribution of factor VIII related antigen and actin has been studied.

With SEM it was possible to detect aspects of carotid plaques not appreciated when using other conventional techniques. With TEM some modifications of the structural and/or functional features of connective tissue macromolecules have been observed. The occurrence of anomalous collagen has been shown.

The fine investigation of endothelial cells, smooth muscle cells and the intercellular matrix components has supplied information of particular morpho-functional significance, thus allowing the development of new ideas on the complex pathogenetic mechanisms of atherosclerosis and suggesting some important anatomo-clinical correlations.

Introduction

Electron microscopy has been already widely used to help clarify intricate pathogenetic mechanisms of atherosclerotic disease. These contributions generally involve transmission (TEM) or scanning electron microscopy (SEM) and have been mainly performed on experimental animals.

At this point we believe that the following two conditions are now indispensable: 1) studies on man; 2) all actual morphological facilities (SEM + TEM and analytical techniques) combinedly applied to the same material.

With such assumptions, we have studied the carotid atheromatous plaque which is undoubtedly an optimum model to investigate atherosclerosis in man. In fact it is the starting-point of one of the most frequent and serious consequences of this disease, cerebral lesion.

The applied techniques, together, provided original dynamic and functional observations. We have been able to confirm previous data and observations (5, 7, 10, 18), deduce some new ideas relating to pathogenetic pathways and to suggest some important anatomo-clinical correlations.

Materials and Methods

Atheromatous plaques were taken from 30 patients (both males and females, between 50 and 60 years, some clinically asymptomatic) submitted to endoarteriectomy for atherosclerotic stenosis localized at the level of carotid bifurcation. Normal control carotids were taken from young persons who died of trauma accidents. All specimens were treated both for SEM and TEM. Semithin sections were used to guide by light microscopy TEM selection. Different cytochemical or immunocytochemical techniques have been applied.

KEY WORDS: Atherosclerosis, carotid atheroma, man, endothelial cells, smooth muscle cells, intercellular matrix, collagen, proteoglycans

Address for correspondence:

R. Laschi

Institute of Clinical Electron Microscopy

University of Bologna

Via Massarenti 9

40138 Bologna, Italy Phone no.: 051 302874

SEM

Each segment of carotid obtained by surgical resection was cut in several parts that were treated as follows: a. some were fixed in glutaraldehyde 3% in 0.1 M sodium cacodylate buffer (pH 7.3, for 3 h at 4°C), dehydrated in a graded series of ethanol, critical point dried and coated with gold by sputtering (30 nm); b. some were fixed in glutaraldehyde 3% in 0.1 M sodium cacodylate buffer (pH 7.3, overnight at 4°C), rinsed with at least 6 changes of 0.1 M sodium cacodylate buffer and left immersed in that buffer overnight at 4°C. Specimens were rinsed for 20 min in distilled water (5 changes) and stained by the silver methenamine method according to Becker and Sogard (1) in order to detect cell nuclei by backscattered electron (BSE) mode. After staining, the specimens were dehydrated in ethanol, critical point dried and coated with a thin layer of gold (10 nm); c. some were fixed with Flickinger's solution (2% formaldehyde and 2.5% glutaraldehyde) containing 0.2% digitonin overnight, according to Scallen and Dietert (17). The specimens were rinsed in 0.05 M sodium cacodylate buffer and postfixed in 1% osmium tetroxide for 5, 10, 20, 30, 60 minutes in order to detect free cholesterol. After post fixation, the specimens were dehydrated in acetone, critical point dried and coated with gold (10 nm); d. specimens for X-ray microanalysis (EDXA) were frozen in nitrogen slush and stored in liquid N<sub>2</sub>, then transferred into a freeze-dryer apparatus (from -100°C to room temperature in 5 days) and coated with a carbon layer (about 30 nm).

All specimens were observed with a Philips 505 scanning electron microscope at 20-30 kV.

TEM

Carotid segments were subdivided transversely to the luminal surface and different specimens fixed by immersion in: a. 2.5% glutaraldehyde in 0.1 M phosphate buffer, postfixed in 1% OsO<sub>4</sub> in veronal buffer, for routine observation; b. 2.5% glutaraldehyde in 0.1 M sodium cacodylate buffer plus 3 mg/ml tannic acid, postfixed in 1% OsO<sub>4</sub> in 0.1 M cacodylate buffer, for detection of elastic fibers; c. 3% glutaraldehyde in 0.1 M cacodylate buffer plus 1 mg/ml ruthenium red, postfixed in 1% OsO<sub>4</sub> in cacodylate buffer plus 1 mg/ml ruthenium red, for detection of proteoglycans; d. 2.5% glutaraldehyde in 0.1 M phosphate buffer, stained with Alcian Blue GX at critical electrolyte concentration (CEC) of 0.3 MgCl<sub>2</sub>, postfixed in 1% OsO<sub>4</sub> in veronal buffer, for glycosaminoglycans detection. In particular chondroitinsulphates A, B, C (chondroitin 4 sulphate, dermatan sulphate, chondroitin 6 sulphate) were demonstrated. As control, prior digestion with

chondroitinase ABC (Sigma) 0.13 U/ml in Tris-HCl buffer, was performed; e. 2% OsO<sub>4</sub> in distilled water plus an equal volume of 5% potassium pyroantimonate, for calcium ions demonstration; f. 2.5% glutaraldehyde - 2% paraformaldehyde plus 0.2% digitonin and 0.05% CaCl<sub>2</sub> in 0.1 M cacodylate buffer, for non esterified cholesterol detection.

All specimens were then dehydrated in a graded series of acetone and embedded in Araldite. Ultrathin (80-100 nm) and semithin (0.5 µm) sections were obtained with an LKB ultratome IV, counterstained with uranyl acetate and lead citrate and observed with a Hitachi H-800 transmission electron microscope, at 100 and 200 kV, in order to achieve best resolution and to attempt on thicker sections a stereological correlation among different components of the extracellular matrix.

Immunocytochemistry

Specimens were fixed in periodate-lysine-paraformaldehyde (PLP) for 6 h at 4°C, dehydrated in graded ethanol and embedded in Araldite.

Antisera. Mouse monoclonal anti-actin was obtained from Amersham International plc(England); rabbit anti-human Factor VIII related antigen (F VIII R:Ag) and rabbit anti-mouse immunoglobulins from Dakopatts A/S (Denmark).

Immunocytochemical labeling. The protein A-gold post-embedding technique (16) was applied on semithin and thin sections. Incubation was carried out as follows:

- mouse monoclonal anti-actin (diluted 1:20,000 in PBS containing 1% ovoalbumin) for 18 h at 4°C in a moist chamber followed by rabbit anti-mouse Ig (diluted 1:20 in the same buffer) for 20 min at room temperature, and protein A- gold complex for 15 min at room temperature;
- rabbit anti-human F VIII R:Ag (diluted 1:500 in the same buffer) for 18 h at 4°C in a moist chamber followed by protein A- gold complex for 15 min at room temperature.

For semithin sections, silver staining (4) was performed after the immunogold reaction. As controls, both PBS or a pre-immune serum instead of specific antisera and incubation with protein A alone were used.

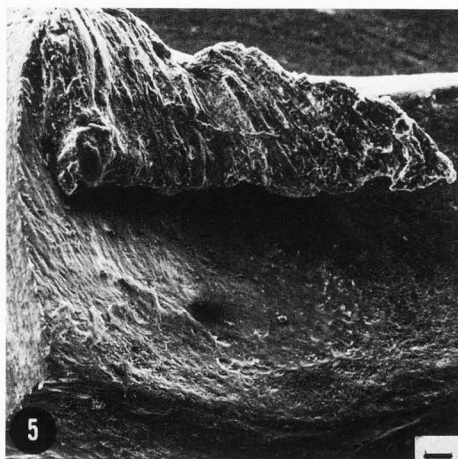
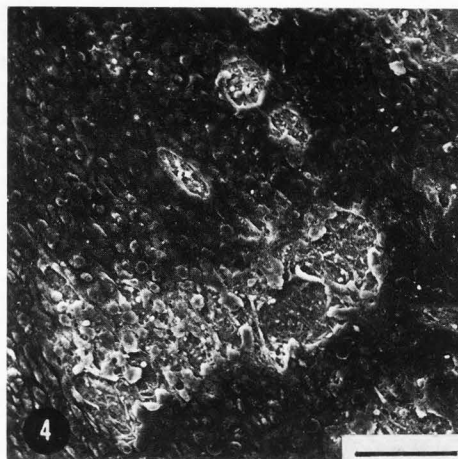
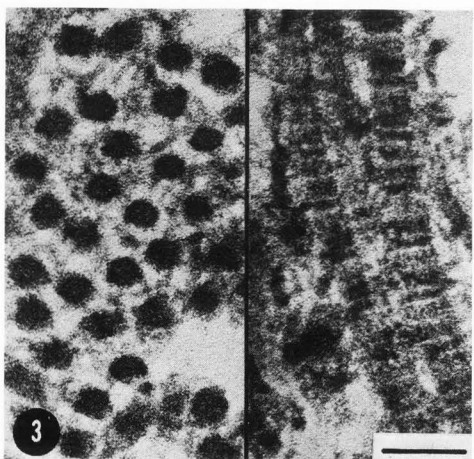
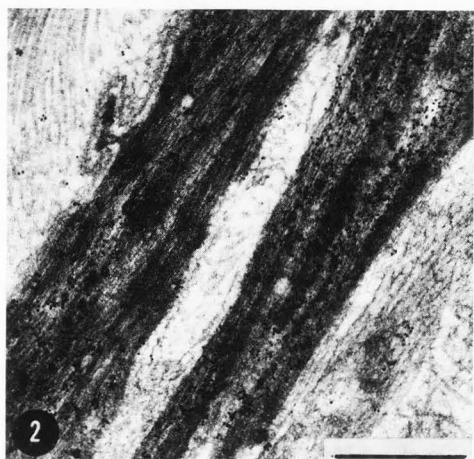
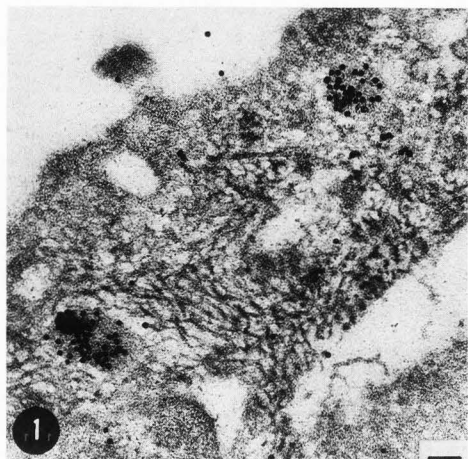
Polychromatic images by equidensitometry

Images were taken by means of a telecamera connected to a Tesak UDC 501 image analyzer both from electron and light micrographs. Equidensitometry of black and white images was performed by assigning to the same intensity zones a given colour, thus obtaining a differential polychromatic image on the telescreen. Such a technique has allowed to detect better some slight differences in density.

Results

Three structures of the arterial wall have been most studied to date: endothelial cells, smooth muscle cells, intercellular matrix components. We also have taken the deepest possible "look" into these structures, taking into consideration that they form complex, integrated functional units.

Normal carotids showed endothelial cells clearly interconnected, characterized by the presence of factor VIII complex detected by indirect method with colloidal gold both on semithin sections by the light microscope and by TEM into Weibel-Palade bodies (Fig. 1). Smooth muscle cells appeared regularly distributed in



Figs. 1 - 3: Normal carotid. Figs. 1,2: Immunogold staining. Bar = 100 nm (Figs. 1,3), and 1  $\mu$ m (Fig. 2).

Fig. 1: Factor VIII complex appears clearly (black granules) into Weibel-Palade bodies.

Fig. 2: Strong positivity for actin into smooth muscle cells.

Fig. 3: Collagen fibers present a regular pattern, both in cross (left) and tangential (right) section.

Figs. 4 and 5: Carotid atheroma. SEM. Bar = 100  $\mu$ m.

Fig. 4: Areas of ripping-off of endothelium.

Fig. 5: Thrombus floating in the lumen.

the media and showed a strong positivity for actin (Fig. 2). Elastic fibers were uniformly stained with tannic acid. Collagen fibers, analysed in detail by TEM at high voltage both in cross and tangential sections, always presented a regular macromolecular pattern (Fig. 3).

The most important and characteristic changes detected in atheromatous carotids were the following:

#### SEM

Observation of areas far from the atheromatous plaque showed a series of lesions that may be correlated to the morphogenesis of the atheromatous formation. Areas of ripping-off of endothelium (Fig. 4), some larger than others, surrounded by swollen endothelial cells with ruptured cell membrane and loss of intercellular junctions were detected. Platelet deposits and red cells often engulfed in fibrin correspond to these areas.

Upon examination the plaques presented accumulations of atheromatous material generally devoid of endothelial lining (aspects of re-endothelialization may only be seen in some areas). Microthrombi varying in shape and size and consisting of fibrin, red cells and platelets in different stages of organization were detected at this level.

All symptomatic patients presented microulcerations varying in diameter from 150 to 300  $\mu\text{m}$ ; these were also visible in some asymptomatic patients. These lesions were usually flat, only rarely were they deep. The surfaces of these lesions consisted of strands of fibrin mixed with red cells and platelets. No difference was observed between the two groups of patients as regards the presence of thrombi. Moreover, in one asymptomatic patient an extended thrombus floating in the lumen was identified which had not resulted at angiography (Fig. 5).

In some cases, probable "loci minoris resistentiae" were detected in the plaque as a consequence of variation in operating conditions. In some points, real microulcerations, evidently covered and therefore masked by a very thin layer of overhanging material (Figs. 6, 7), were in fact evidenced by increasing the observation voltage (from 5/8 keV to 20/25 keV) as well as the electron beam diameter (spot from 50 to 200 nm).

In some cases when the specimen was cryo-fractured along the plaque thickness, numerous round shaped canalicular orifices appeared in cross section (Fig. 8). They were, as confirmed by transmission electron microscopy and by immunocytochemistry at light microscopy on semithin sections, very small newly formed vessels, surrounded by microhemorrhages.

Extensive bands of lipid material, constantly in the subendothelium, were revealed by BSE mode (Fig. 9); these would not have been otherwise visible. Dome-shaped mounds, apparently due to the presence of large cells full of lipids (foam cells), were sometimes observed on the plaque surface towards the lumen.

Examination of the plaques of some patients by means of X-ray microanalysis in SEM showed that the ratio of calcium to phosphorous was significantly higher compared to controls.

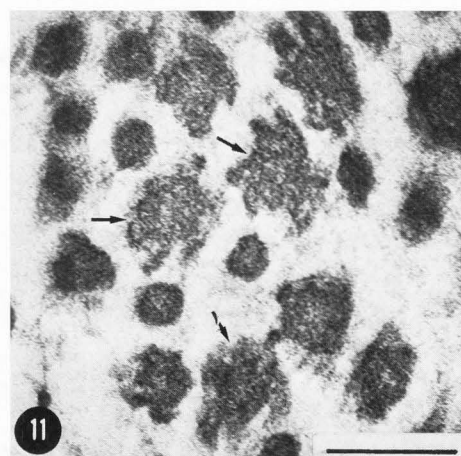
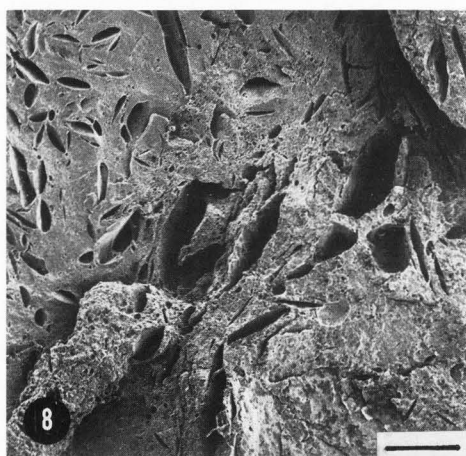
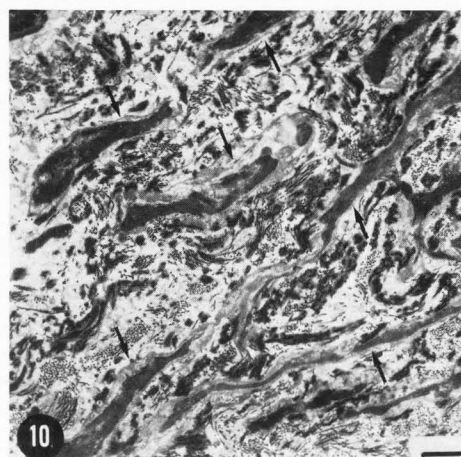
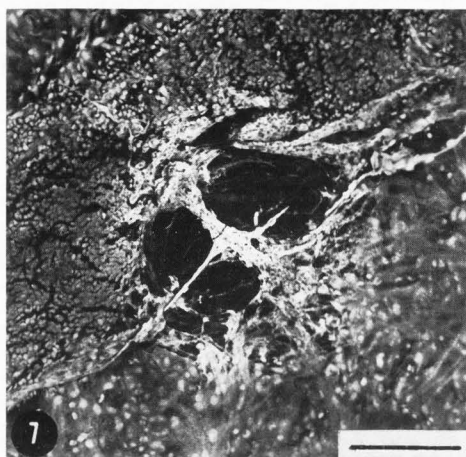
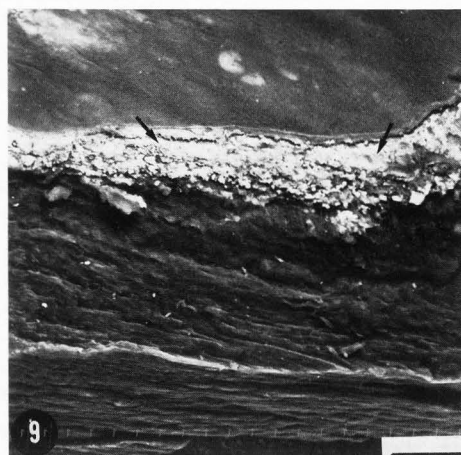
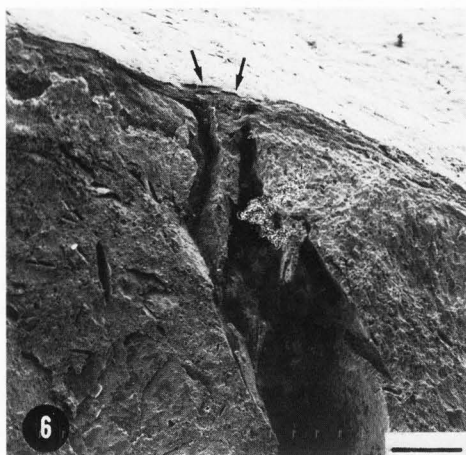
#### TEM

Elastic fibers. The elastic material, easily identifiable by tannic acid staining, is apparently composed of medium electron-dense laminae, often interrupted by large gaps: the extremities of the laminae in these discontinuities show a progressive reduction in electron-density and a change in their morphology (Fig. 10), from a compact lamina to a reticular structure in whose meshwork low electron-dense flaky material and lipid droplets may be observed. Accumulations of positive tannic acid material are randomly and irregularly distributed.

Collagen. Inside the intima, especially in cases of advanced fibrosis, numerous collagen fibrils may be observed, often packed together or more often isolated without orientation. The diameter of the fibrils appears generally uniform except in fairly well defined areas in which peculiar shaped fibrils with large diameters may be observed next to the smaller ones. These larger fibrils in cross section show roughly an irregular outline with more or less deep indentations which may modify almost completely the fibril structure thus putting into evidence the microfibrillar arrangement (Fig. 11). These structures "flower-like" or "hieroglyphic-shaped" when observed in longitudinal sections, confirm the fibril dissociation into subfibril unities (Fig. 12) still maintaining a regular band-type arrangement. The "abnormal" collagen often appears to be associated with cell elements which themselves appear to have intermediate organellar characteristics between smooth muscle cells and fibroblastic-type cells.

Proteoglycans. In the specimens treated with ruthenium red, numerous granules are visible. These are dispersed in the extracellular matrix and most probably consist of proteoglycans. They appear tied to one another by low electron-density filamentous structures in order to form a tight meshwork. These thin filaments may also be seen as narrow bridges between adjacent collagen fibrils or arranged over the same fibrils in almost periodic pattern. A dense population of small granules also delimits the elastic fibre outlines.

Carotid atheroma in man



Figs. 6-11: Carotid atheroma. SEM (Figs. 6-9, bar = 100  $\mu$ m); TEM (Fig. 10, bar = 1  $\mu$ m; Fig. 11, bar = 100nm).

Fig. 6: Ulceration covered, towards the lumen, by a thin layer of material (arrows).

Fig. 7: Microulcerations (with threads of fibrin) evidenced by increasing the observation voltage.

Fig. 8: Numerous newly formed vessels along the plaque thickness.

Fig. 9: Extensive subendothelial band of lipids (arrows), revealed by BSE mode.

Fig. 10: Tannic acid. Fragmented laminae of elastic material (arrows) among collagen fibrils.

Fig. 11: Anomalous "flower-like" (arrows) collagen fibers in cross section.

In the specimens stained with Alcian Blue, numerous rather thick electron-dense filaments are observed in the spaces without collagen fibrils (Fig. 13). These filaments form a tight meshwork probably representing proteoglycan aggregates containing chondroitin sulphates (ChS, A, B, C). Moreover, shorter and thinner filaments (dermatan sulphate) appear associated to the collagen fibrils and to the elastic ones. The thick extrafibrillar meshwork and the interfibrillar filaments almost completely disappear after digestion with chondroitinase ABC and Alcian Blue staining whereas long and thin filaments probably composed of heparan sulphate or keratan sulphate, remain in the extrafibrillar areas.

Lipids. Numerous lipid droplets with intracellular localization are present in the foam cells (Fig. 14): some seem to contain non esterified cholesterol due to a positive reaction with digitonin (Fig. 15). Intracellular lipids may also take the form of large crystals on whose surfaces numerous primary lysosomes may frequently be observed. In the extracellular environment, free lipid droplets packed together often seem to substitute, almost completely, the extracellular matrix.

Calcium. The specific reaction for calcium ion detection shows the presence, especially in some cases, of numerous very electron-dense precipitates (Fig. 16). They are in the extracellular matrix, taking the form of round-shaped particles associated to the fragmented elastic fibers, or inside certain macrophagic-type cells often contained in large lysosomal vacuoles, or in smooth muscle cells along the myofilaments. Often intercellular calcium ion deposits appear to be associated with numerous lipid droplets.

#### Immunocytochemistry

The specific immunological staining for the factor VIII regularly visible in the cytoplasm of normal endothelial cells disappeared in areas with ripped-off endothelium. Weak staining for this antigen delimited the outline of the vascular newly formed structures present in the thickened intima.

The immunological reaction for actin detection showed minor intensity in the smooth muscle cells transformed into fibroblast-like cells migrated in the thickened intima (Fig. 17), compared to the normal smooth muscle cells of the media.

#### Discussion

All recent theories concerning the pathogenesis of atherosclerosis describe two main alterations detectable at the morphological level, represented by proliferation and migration of smooth muscle cells and deposition of intracellular and extracellular lipids.

It is generally felt that the smooth muscle cell is the "superstar" of atherogenesis due to

its particular reactivity to physiological and pathological stimulations (3). The activation of smooth muscle cells triggers a series of modulations (initially quite rhythmic and coordinated, later partly "off-key") which characterize the whole focal symphony of atherosclerosis (9). Lysosomal traffic into their lipoprotein-filled cytoplasm, transformation into fibroblast-like cells, metabolic modifications with changed synthetic abilities, secretion of new macromolecular components of the extracellular matrix are some of the different steps discussed and stressed. The deepest study of the relationships between smooth muscle cells and matrix (2, 19) may certainly contribute to clear the pathogenesis of the disease keeping in mind how much early changes in extracellular environment may influence cell activity and viceversa (8, 11, 12, 13, 14).

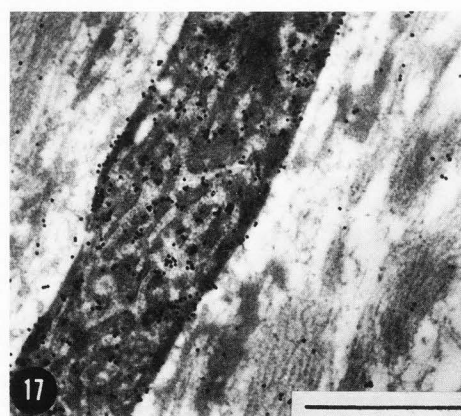
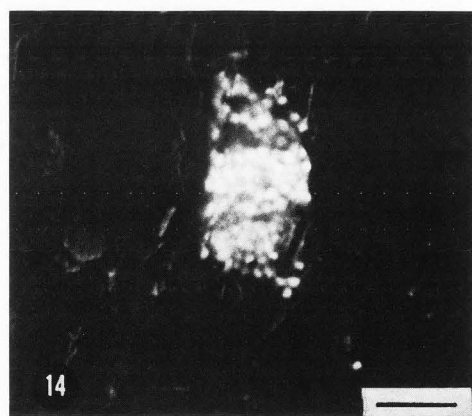
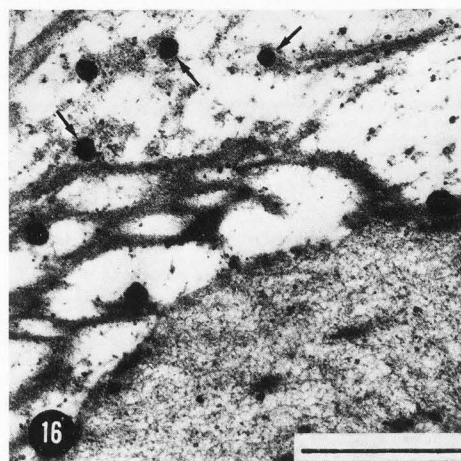
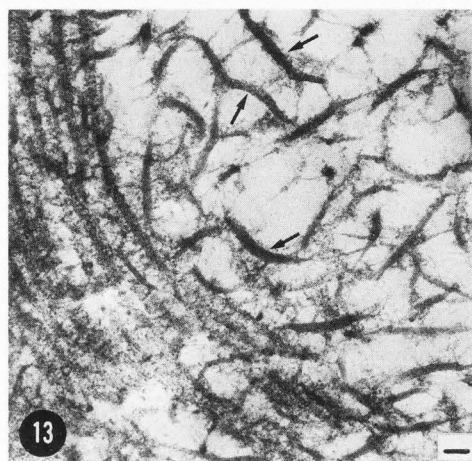
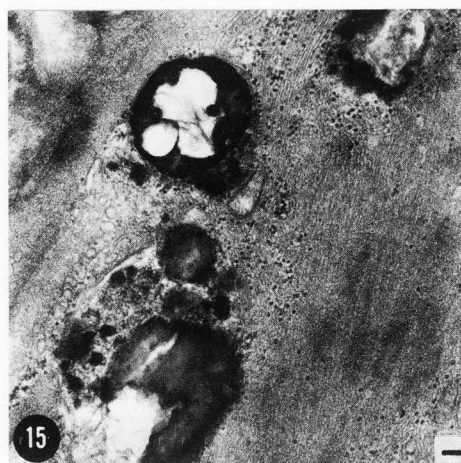
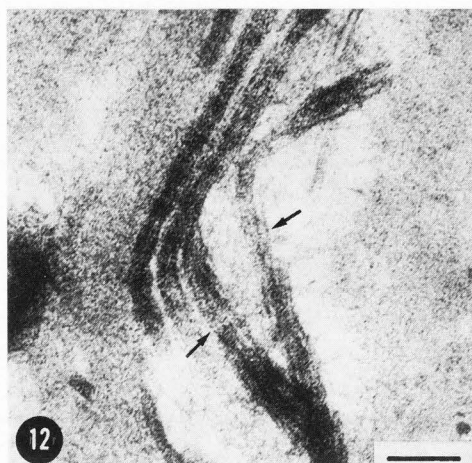
Our contribution to the study of carotid atheroma in man is among the first to be carried out in detail with the use of comparative and correlative modern morphological techniques. Steps in the evolution of the atherosclerotic process, through changes both of cells and of different components of the extracellular matrix, have been further demonstrated.

Defining the step beyond which plaque evolution in man becomes irreversible is a very fundamental practical point. One of the markers we have checked in our material that seems to indicate the impossibility, or at least the great difficulty of regression of the plaque is likely represented by the deposition of anomalous collagen. This "collagen dysplasia" has been observed also in genetic collagen diseases (6, 15) (as Ehler-Danlos, Marfan, Osteogenesis Imperfecta) and could signify a final common pathway at the morphological level, derived from anomalous processes at the biochemical level or during the synthesis of collagen fibrils or in the post-synthetic phase. Thus, a future pharmacological prospective might be controlling the cell synthesis of such macromolecules.

In some of our patients angiography was negative for ulcerations; however SEM analysis showed "masked" microulcerations which justify surgical intervention. Also in asymptomatic patients we always observed aspects predicting plaque evolution. Moreover SEM has shown very clearly the development of new vessels within the atheromatous plaque. This explains the frequent hemorrhages.

In conclusion, our data suggest that once an atheromatous plaque reaches a given step it seems to have no possibility of reversibility. This may also apply to fairly young and asymptomatic patients, who are negative to some parameters at routine morpho-clinical investigation.

Carotid atheroma in man



Figs. 12 - 17: Carotid atheroma. Figs. 12, 13, 15, 16 - TEM; Fig. 14 - SEM; Fig. 17 - Immunogold staining.

Fig. 12: Fibril dissociation (arrows) of anomalous collagen. Bar = 100 nm.

Fig. 13: Alcian Blue. Thick filaments of proteoglycans (arrows). Bar = 100 nm.

Fig. 14: Intracellular localization of lipids visible by BSE mode. Bar = 10  $\mu$ m.

Fig. 15: Digitonin reaction shows the presence of non esterified cholesterol (dense areas) in lipid droplets. Bar = 100 nm.

Fig. 16: Potassium pyro-antimonate. Calcium electron-dense precipitates (arrows). Bar = 1  $\mu$ m.

Fig. 17: Minor positivity for actin into transformed smooth muscle cells migrated into the thickened intima, compared to the normal smooth muscle cells. Bar = 1  $\mu$ m.

Further studies of fine cellular and subcellular processes will suggest pharmacological intervention, but at earlier phases which we may, in the future, be able to define before they reach the point of no-return.

#### References

1. Becker RP, Sogard M (1979). Visualization of subsurface structures in cells and tissues by backscattered electron imaging. *Scanning Electron Microsc*, 1979; II: 835-870.
2. Burke JL, Ross R (1979). Synthesis of connective tissue macromolecules by smooth muscle. *Int Rev Connect Tissue Res*, 8, 119-157.
3. Campbell GR, Chamley-Campbell JH (1981). The cellular pathobiology of atherosclerosis. *Pathology*, 13, 423-440.
4. Danscher G, Nørgaard JOR (1983). Light microscopic visualization of colloidal gold on resin-embedded tissue. *J Histochem Cytochem*, 31, 1394-1398.
5. Hertzner NR, Beven EG, Benjamin SP (1977). Ultramicroscopic ulcerations and thrombi of the carotid bifurcation. *Arch Surg*, 112, 1394-1402.
6. Holbrook KA, Byers PH (1982). Structural abnormalities in the dermal collagen and elastic matrix from the skin of patients with inherited connective tissue disorders. *J Invest Dermatol*, 79, 7s-16s.
7. Hushang J (1979). Development of carotid plaque. *Am J Surg*, 138, 224-227.
8. Katsuda S, Nakanishi I, Kajikawa K, Kitamura T (1983). Elastolysis following partial constriction of the common carotid arteries of rabbits. *J Electron Microsc*, 32, 45-53.
9. Laschi R (1982). Atherosclerosis in man. *Atlas of electron microscopy*. Ed. Skema-Compositori, Bologna.
10. Lusby RJ, Ferrell LD, Ehrenfeld WK, Stoney RJ, Wylie EJ (1982). Carotid plaque hemorrhage. Its role in production of cerebral ischemia. *Arch Surg*, 117, 1479-1487.
11. McCullagh KG (1983). Increased type I collagen in human atherosclerotic plaque. *Atherosclerosis*, 46, 247-248.
12. Morton LF, Barnes MJ (1982). Collagen polymorphism in the normal and diseased blood vessel wall. *Atherosclerosis*, 42, 41-51.
13. Ooshima A (1981). Collagen  $\alpha$  B chain: increased proportion in human atherosclerosis. *Science*, 213, 666-668.
14. Picard J, Breton M, Deudon E (1979). Le rôle des protéoglycanes de la paroi artérielle dans l'athérosclérose. *Sem Hôp Paris*, 55, 748-752.
15. Pope FM, Dorling J, Nicholls AC, Webb J (1983). Molecular abnormalities of collagen: a review. *J Royal Soc Med*, 76, 1050-1062.
16. Roth J, Bendayan M, Orci L (1978). Ultrastructural localization of intracellular antigens by the use of Protein A-gold complex. *J Histochem Cytochem*, 26, 1074-1081.
17. Scallen TJ, Dietert SE (1969). The quantitative retention of cholesterol in mouse liver prepared for electron microscopy by fixation in a digitonin-containing aldehyde solution. *J Cell Biol*, 40, 802-813.
18. Smith RR, Russell WF, Percy ML (1980). Ultrastructure of carotid plaques. *Surg Neurol*, 14, 145-153.
19. Staubesand J, Fischer N (1980). The ultrastructural characteristics of abnormal collagen fibrils in various organs. *Connect Tissue Res*, 7, 213-217.

#### Discussion with Reviewers

W.G. Jerome: In both animal models of atherosclerosis and in human lesions, monocyte derived macrophages have been implicated in both progression and regression of the lesion. Have you seen any evidence of monocytes in the lesions you have studied?

Author: We have seen very few monocyte-like cells. Most probably this is due to the fact that the human lesions we have studied, obtained during surgical endoarterectomy, were all fairly advanced.

W.G. Jerome: It has been well established that surgical procedures and critical point drying can produce artifactual denudation such as that presented in fig.4. Since numerous light and transmission electron microscopic studies have failed to document this type of gross denudation in either human or animal arteries, why does the author feel these areas in their preparation are not artifactually produced?  
Author: Nobody can exclude that they may be artifactually produced, but our entire observations performed on different points make us think they probably represent the first lesions of the arterial wall.

R. Albrecht: The areas in figure 4 referred to as being correlated to the morphogenesis of the atheromatous formation seem extensive. Does the author feel these are "reversible" lesions that, if treated or prevented, would reduce the incidence of plaque formation?

Author: We feel that these lesions may be reversible and, if treated, plaque formation may be prevented.